Transcriptomics unveils immune metabolic disruption and a novel biomarker of mortality in patients with HBV-related acute-on-chronic liver failure

Authors

Xi Liang, **Peng Li**, **Jing Jiang**, **Jiaojiao Xin**, Jinjin Luo, Jiaqi Li, Pengcheng Chen, Keke Ren, Qian Zhou, Beibei Guo, Xingping Zhou, Jiaxian Chen, Lulu He, Hui Yang, Wen Hu, Shiwen Ma, Bingqi Li, Xin Chen, Dongyan Shi, Jun Li

Correspondence

lijun2009@zju.edu.cn (J. Li), shidongyan@zju.edu.cn (D. Shi).

Graphical abstract

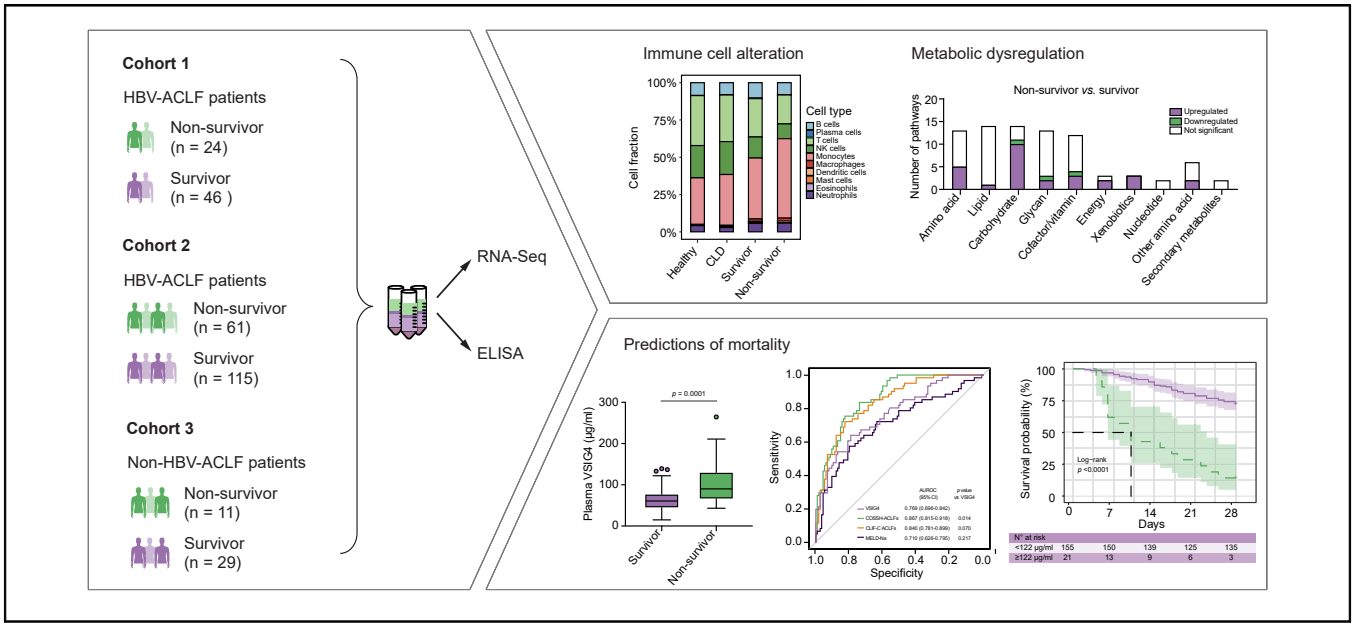

Highlights

- Dysregulation of monocytes, CD8+ T cells and NK cells was highly correlated with 28-day mortality in patients with HBV-ACLF.
- The association of metabolic heterogeneity and reprogramming with outcomes in HBV-ACLF was systematically characterized.
- VSIG4, a macrophage complement receptor, was highly expressed in patients with poor outcomes.
- Risk stratification of the plasma VSIG4 level (>122 μg/ml) specifically identified patients with a high risk of death.
- The generality of VSIG4 in patients with ACLF of other etiologies was validated.

Impact and implications

Acute-on-chronic liver failure (ACLF) is a lethal clinical syndrome associated with high mortality. We found significant immune cell alterations and metabolic dysregulation that were linked to high mortality in patients with HBV-ACLF based on transcriptomics using peripheral blood mononuclear cells. We identified VSIG4 (V-set and immunoglobulin domain-containing 4) as a diagnostic and prognostic biomarker in ACLF, which could specifically identify patients with ACLF at a high risk of death.

https://doi.org/10.1016/j.jhepr.2023.100848

Research article

JHEP|Reports

Transcriptomics unveils immune metabolic disruption and a novel biomarker of mortality in patients with HBV-related acute-on-chronic liver failure

Xi Liang,[1,2,†] **Peng Li**,[2,†] **Jing Jiang**,[2,†] **Jiaojiao Xin**,[2,†] Jinjin Luo,[2] Jiaqi Li,[2] Pengcheng Chen,[3] Keke Ren,[2] Qian Zhou,[2] Beibei Guo,[2] Xingping Zhou,[2] Jiaxian Chen,[2] Lulu He,[2] Hui Yang,[2] Wen Hu,[2] Shiwen Ma,[2] Bingqi Li,[2] Xin Chen,[4,5] Dongyan Shi,[2,*] Jun Li [1,2,*], on behalf of Chinese Group on the Study of Severe Hepatitis B (COSSH)

[1]Precision Medicine Center, Taizhou Central Hospital (Taizhou University Hospital), Taizhou, 318000, China; [2]State Key Laboratory for Diagnosis and Treatment of Infectious Diseases, National Clinical Research Center for Infectious Diseases, National Medical Center for Infectious Diseases, The First Affiliated Hospital, Zhejiang University School of Medicine, Hangzhou, 310003, China; [3]Institute of Big Data and Artificial Intelligence in Medicine, School of Electronics and Information Engineering, Taizhou University, Taizhou, China; [4]Institute of Pharmaceutical Biotechnology and the First Affiliated Hospital, Department of Radiation Oncology, Zhejiang University School of Medicine, Hangzhou, China; [5]Joint Institute for Genetics and Genome Medicine between Zhejiang University and University of Toronto, Zhejiang University, Hangzhou, China

JHEP Reports **2023.** https://doi.org/10.1016/j.jhepr.2023.100848

Background & Aims: HBV-related acute-on-chronic liver failure (HBV-ACLF) is a complex syndrome associated with high short-term mortality. This study aims to reveal the molecular basis and identify novel HBV-ACLF biomarkers.
Methods: Seventy patients with HBV-ACLF and different short-term (28 days) outcomes underwent transcriptome sequencing using peripheral blood mononuclear cells. Candidate biomarkers were confirmed in two external cohorts using ELISA.
Results: Cellular composition analysis with peripheral blood mononuclear cell transcriptomics showed that the proportions of monocytes, T cells and natural killer cells were significantly correlated with 28-day mortality. Significant metabolic dysregulation of carbohydrate, energy and amino acid metabolism was observed in ACLF non-survivors. V-set and immunoglobulin domain-containing 4 (*VSIG4*) was the most robust predictor of patient survival (adjusted $p = 1.74 \times 10^{-16}$; variable importance in the projection = 1.21; AUROC = 0.89) and was significantly correlated with pathways involved in the progression of ACLF, including inflammation, oxidative phosphorylation, tricarboxylic acid cycle and T-cell activation/differentiation. Plasma VSIG4 analysis externally validated its diagnostic value in ACLF (compared with chronic liver disease and healthy groups, AUROC = 0.983). The prognostic performance for 28-/90-day mortality (AUROCs = 0.769/0.767) was comparable to that of three commonly used scores (COSSH-ACLFs, 0.867/0.884; CLIF-C ACLFs, 0.840/0.835; MELD-Na, 0.710/0.737). Plasma VSIG4 level, as an independent predictor, could be used to improve the prognostic performance of clinical scores. Risk stratification based on VSIG4 expression levels (>122 μg/ml) identified patients with ACLF at a high risk of death. The generality of VSIG4 in other etiologies was validated.
Conclusions: This study reveals that immune-metabolism disorder underlies poor ACLF outcomes. VSIG4 may be helpful as a diagnostic and prognostic biomarker in clinical practice.
Impact and implications: Acute-on-chronic liver failure (ACLF) is a lethal clinical syndrome associated with high mortality. We found significant immune cell alterations and metabolic dysregulation that were linked to high mortality in patients with HBV-ACLF based on transcriptomics using peripheral blood mononuclear cells. We identified VSIG4 (V-set and immunoglobulin domain-containing 4) as a diagnostic and prognostic biomarker in ACLF, which could specifically identify patients with ACLF at a high risk of death.

Keywords: acute-on-chronic liver failure; transcriptomics; biomarker; mortality; V-set and immunoglobulin domain-containing 4.
Received 20 November 2022; received in revised form 16 June 2023; accepted 1 July 2023; available online 17 July 2023
† These authors contributed equally to this work.
* Corresponding authors. Addresses: Precision Medicine Center, Taizhou Central Hospital (Taizhou University Hospital), Taizhou, 318000, China. State Key Laboratory for Diagnosis and Treatment of Infectious Diseases, National Clinical Research Center for Infectious Diseases, National Medical Center for Infectious Diseases, The First Affiliated Hospital, Zhejiang University School of Medicine, Hangzhou, 310003. China. Tel: 86- 571-87236425; fax: 86-571-87236425 (D. Shi) (J. Li).
E-mail addresses: lijun2009@zju.edu.cn (J. Li), shidongyan@zju.edu.cn (D. Shi).

Introduction

HBV-related acute-on-chronic liver failure (HBV-ACLF) is a complicated syndrome that develops in patients with HBV-related chronic liver disease and is characterized by acute deterioration of liver function and multiple extrahepatic organ failures.[1,2] The progression of HBV-ACLF is rapid, and the short-term mortality rate remains as high as 50%–90% despite intensive treatments.[1,3] Early diagnosis and accurate prognostication are important for improving survival. Recently, many studies have mainly focused on developing prognostic scores based on clinical indicators. The

European Association for the Study of the Liver-Chronic Liver Failure (EASL-CLIF) Consortium and the Chinese Group on the Study of Severe Hepatitis B (COSSH) both developed prognostic scores based on the sequential assessment of six types of organ failures, the CLIF-C ACLF score and the COSSH-ACLF score, respectively.[1,4] Subsequently, the COSSH study proposed a simplified version of the score (the COSSH-ACLF II score) with higher prognostic accuracy and sensitivity for patients with HBV-ACLF, and the score easily stratified patients into three risk groups with significantly different short-term mortality rates.[5] Although these scores are widely used for decision-making in patients with ACLF of different etiologies, they are not easily used for bedside assessment based on the combination of various criteria of six types of organ failures or complicated calculations with many different variables, and the diagnosis and prognostication are comparably late with insufficient time for intensive care.

To date, the molecular mechanisms of ACLF in patients with different outcomes remain unclear.[6–8] Studies from the EASL-CLIF Consortium have emphasized that systemic inflammation plays an important role in ACLF progression and development via analysis of circulating cytokines in patients with alcohol-related etiology.[6] The COSSH study indicated that immune-metabolism disorder is a core axis of disease progression and development in patients with HBV-ACLF.[8] The identification of potential molecular biomarkers associated with the diagnosis and prognosis of ACLF remains an unmet need.

The identification of sensitive and specific biomarkers underlying the molecular mechanisms of progression and outcomes in ACLF is needed to help with the early diagnosis of the condition and to improve our understanding of its complex pathophysiology. In this study, we performed transcriptome sequencing using peripheral blood mononuclear cells (PBMCs) from patients with HBV-ACLF and chronic liver diseases to reveal the pathophysiology and identify potential biomarkers associated with poor HBV-ACLF outcomes.

Materials and methods

Study design

To characterize the pathophysiological variations that underlie short-term (28 days) ACLF outcomes, 246 patients with HBV-ACLF and different short-term outcomes (died within 28 days: non-survivor, n = 85; survived within 28 days: survivor, n = 161) were enrolled from the prospectively maintained COSSH study.[1,3,5] Patients with cirrhosis and chronic hepatitis B (CHB) were enrolled as chronic liver disease (CLD) controls. Healthy volunteers were enrolled as normal controls. As shown in Fig. 1A, cohort 1 (sequencing cohort: ACLF non-survivor, n = 24; ACLF survivor, n = 46; CLD, n = 20; healthy, n = 15) was used to reveal the pathophysiology and biomarkers associated with poor ACLF outcomes. Cohort 2, comprising 61 ACLF non-survivors, 115 ACLF survivors, 70 patients with CLD and 35 healthy controls, was enrolled to confirm potential biomarkers for the diagnosis and prognosis of HBV-ACLF by ELISA. Stratified random sampling according to the prevalence of ACLF grades in the COSSH study was performed to enroll the sequencing and ELISA cohorts. To further validate the generality of biomarkers in ACLF, 40 patients with non-HBV-related ACLF (non-HBV-ACLF: non-survivor, n = 11; survivor, n = 29) were enrolled in validation cohort 3. Blood samples were all collected at the time of admission (within the first 24 h). Relevant clinical, demographic, laboratory and follow-up data were collected from the electronic data capture system and case report forms. Patients were administered antiviral nucleoside analogs for HBV according to the Consensus Recommendations of the Asian Pacific Association for the Study of the Liver (2009).[9] The study protocol was approved by the Clinical Research Ethics Committee of the First Affiliated Hospital, Zhejiang University School of Medicine (No. 2016-31). All patients were well informed, and written consent was obtained from them or their legal surrogates before enrollment.

Definitions

HBV-ACLF and non-HBV-ACLF

HBV-ACLF was diagnosed when patients met the criteria defined in the COSSH study.[1] The definition identified HBV-ACLF as a complicated syndrome with a high short-term mortality rate that develops in patients with HBV-related chronic liver disease, regardless of the presence of cirrhosis, and is characterized by acute deterioration of liver function and hepatic and/or extrahepatic organ failure. HBV-ACLF comprises three grades: ACLF-1, ACLF-2 and ACLF-3. ACLF-1 comprises four types of patients: (1) patients presenting with liver failure alone with an international normalized ratio (INR) ≥1.5 and/or kidney dysfunction (creatinine

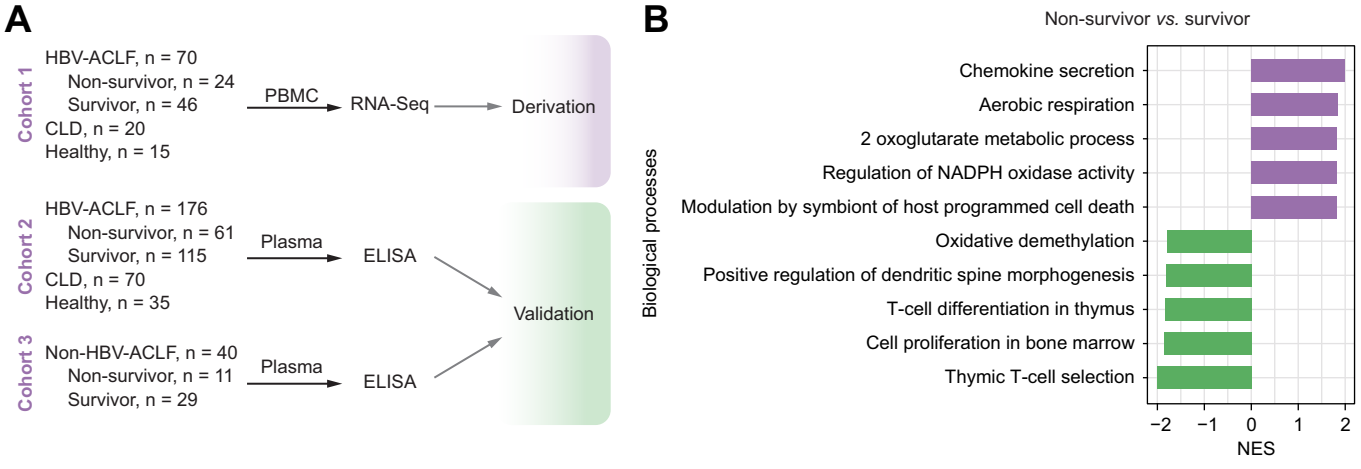

Fig. 1. Study design and transcriptomic characteristics related to poor ACLF outcomes at 28 days. (A) Study design for molecular basis analysis and biomarker development. (B) Gene set-enrichment analysis results of ACLF non-survivors and survivors. The selected 10 significantly enriched gene ontology biological processes are shown. ACLF, acute-on-chronic liver failure; CLD, chronic liver disease; HBV-ACLF, HBV-related ACLF.

levels ranging from 1.5 to 1.9 mg/dl) and/or hepatic encephalopathy (HE) grade I or II; (2) patients with kidney failure (creatinine levels ≥2 mg/dl) alone; (3) patients with failure of a single organ in the coagulation, circulatory or respiratory system and/or kidney dysfunction and/or HE grade I or II; and (4) patients with cerebral failure plus kidney dysfunction. ACLF-2 comprises patients with failures in two organ systems, while ACLF-3 comprises patients with failures in three or more organ systems.

Patients with non-HBV-ACLF etiologies, including alcohol-related liver diseases, autoimmune hepatitis and primary biliary cholangitis, were diagnosed according to EASL-ACLF criteria.[10]

Cirrhosis, CHB and healthy controls

Cirrhosis was defined as patients with stable compensated cirrhosis, which was diagnosed on the basis of previous liver biopsy results, clinical evidence, laboratory tests, and endoscopic (esophageal and gastric varices) and radiological imaging of portal hypertension and/or liver nodularity, as described previously.[8] The etiology of all patients with cirrhosis was HBV-related. Patients with a history of decompensation (ascites/HE/upper gastrointestinal hemorrhage/bacterial infection) were excluded. CHB was defined according to the 2009 American Association for the Study of Liver Diseases guidelines.[11] In the current study, cirrhosis and CHB were combined as the CLD group. Heathy controls were participants with a normal physical examination.

Sample preparation and mRNA sequencing

PBMCs were isolated from whole-blood samples as described in a previous study.[8] Briefly, PBMCs were collected from patients and volunteers using Ficoll-Paque™ PLUS medium (GE Healthcare, Uppsala, Sweden) and washed with DPBS, and total RNA was extracted using TRIzol reagent (Ambion, Carlsbad, CA). The plasma layer from density gradient separation was also collected and stored at -80 °C. Purified RNA was used for sequencing library preparation using the TruSeq® RNA LT Sample Prep Kit v2 according to the manufacturer's instructions (Illumina, San Diego, CA), including adapter ligation, reverse transcription, PCR amplification and pooled gel purification steps. The TruSeq RNA Kit captures the coding transcriptome (without strand information) by using oligo-dT beads complementary to poly-A tails. The pooled library consists of sequences with lengths of approximately 250 nucleotides. mRNA sequencing was performed on a HiSeq 2500 sequencing system (Illumina, United Kingdom).

mRNA-Seq analysis

Raw paired-end sequencing reads were quality controlled using FastQC.[12] Trimmomatic v0.36 was used to remove adaptors and low-quality reads with default parameters.[13] The filtered reads from each sample were aligned to the human reference genome (GRCh38.87) using HISAT v2.0.5 with default settings.[14] HTSeq was used to compute the gene-level counts of each gene based on the mapped and aligned reads with default parameters.[15] Based on the Ensembl human gene annotations of GRCh38, 19,966 protein-coding genes were included. Non-coding genes and other gene locus types were excluded from the present study. Samples for mRNA-Seq were sex-matched among cohorts to prevent sex chromosome gene–associated effects. Raw counts were normalized using the DESeq method in the DESeq2 package v1.14.1 to remove library-specific artifacts.[16] Low-variance genes were removed if their expression variance was <1.0 across samples. A total of 18,789 expressed genes were identified in the sequencing cohort. Batch effects were removed using the ComBat method in the sva package. A detailed description of the differential expression analysis, principal component analysis (PCA), metabolic profile analysis and evaluation of the use of candidate genes for patient discrimination is provided in the supplementary methods.

Immune cellular fraction estimation

To infer the composition of immune cells in PBMCs, CIBERSORTx deconvolution analysis was performed based on the normalized gene counts, with quantile normalization disabled, and 1,000 permutations.[17,18] Samples that had a *p* value for deconvolution <0.05 were considered to deconvolute successfully. Cell signature matrixes were the original 22 immune cell reference profiles of file LM22. The results of 22 immune cell subtypes were summarized into 10 major immune cell types. Five hundred permutations were performed to calculate the *p* value for the significance analysis. The total B-cell population was found by combining the fractions of naïve B cells and memory B cells. The total T-cell population was found by combining the fractions of CD8 T cells, naïve CD4 T cells, resting memory CD4 T cells, activated memory CD4 T cells, follicular helper T cells, regulatory T cells and gamma delta T cells. The total natural killer (NK) cell population was found by combining the fractions of resting NK cells and activated NK cells. The total macrophage population was found by combining the fractions of M0 macrophages, M1 macrophages and M2 macrophages. The total dendritic cell population was found by combining the fractions of resting dendritic cells and activated dendritic cells. The total mast cell population was found by combining the fractions of resting mast cells and activated mast cells.

Functional enrichment analysis

Different approaches were used to identify the changed biological pathways during disease progression.

Gene set variation analysis

To quantify the pathway enrichment score on a single-sample basis, gene set variation analysis (GSVA) was performed using the function gsva in the R package GSVA.[19] Gene ontology biological processes, KEGG metabolic pathways, blood transcriptional modules[20] and whole-blood modules[21] were used as functional annotations for GSVA. To find associations between pathways and disease groups, a linear model was fitted, and empirical Bayes moderated statistics were calculated based on the pathway enrichment scores using the limma package. *P* values were adjusted using the Benjamini–Hochberg procedure. Significance was defined as an adjusted p value of <0.05. Pearson correlation analysis between the single-sample enrichment scores of each pathway and the target gene expression level was conducted using the cor function.

Gene set-enrichment analysis

To illustrate biological states and functional differences during disease progression, gene set-enrichment analysis (GSEA) was performed using pre-ranked analysis based on gene expression.[22] The significance criterion used for GSEA was a *p* value of <0.05. The normalized enrichment score was calculated by GSEA to compare the degree of enrichment across gene sets. GSEA was performed for biological pathways using the gene ontology biological process and KEGG metabolic pathway gene sets in the

MSigDB (Molecular Signature Database)[23] and the blood transcriptional module and whole-blood module gene sets. The significance criterion used for GSEA was a p value of <0.05. Frequency analysis was performed to quantify the percentage of significantly upregulated and downregulated genes in a gene set.

Risk stratification

To identify the optimal cut-off value of the VSIG4 expression level to stratify patients into low- and high-risk of death groups, X-tile software was used.[24] The thresholds were defined as the value that produced the largest χ^2 value in the Mantel–Cox test. Survival analysis was performed using the Kaplan–Meier method, and the log-rank test was used to examine the significance of differences between the low-risk and high-risk groups.

qRT–PCR and ELISA

The *VSIG4* expression level was measured by quantitative reverse-transcription PCR (qRT–PCR) and ELISA. qRT–PCR was performed using a two-step protocol with specific primers, TB Green DYE II (Takara, Beijing, China), and an ABI 7500HT instrument (Thermo Fisher, Waltham, MA) according to the manufacturer's instructions. The amount of cDNA was optimized so that the amplification of both control genes and cDNAs of interest was in the exponential phase. Transcripts were quantified using the comparative Ct method and normalized to the levels of the endogenous control (*GAPDH*). The primers were 5'-TCCTGGAAGTGCCAGAGAGT-3' (sense) and 3'-CTTTGC CTGCTGGATATGGT-5' (antisense) for *VSIG4* and 5'- CTCTCTG CTCCTCCTGTTCG -3' (sense) and 3'- ACGACCAAATCCGTTGACTC -5' (antisense) for *GAPDH*. ELISA was performed using commercially available kits (Human VSIG4 ELISA kit, ELH-VSIG4-1, RayBiotech, Norcross, GA) according to the manufacturer's instructions.

Statistical analysis

Student's t test, the Mann–Whitney U test and the Kruskal–Wallis test were used to compare continuous variables where appropriate. The Shapiro–Wilk test was used to confirm whether the values followed a normal distribution. The $\chi 2$ test and Fisher's exact test were applied to compare categorical variables. The results are presented as the mean ± SD, median [Q1-Q3] or percentages (numbers) unless indicated otherwise. Correlation analysis was conducted with Pearson's correlation. A two-sided p value <0.05 was considered statistically significant. No sample-size calculations were performed. Statistical significance can be derived from the results, representing sufficient power using the given sample size. All statistical analyses were performed with R software (http://www.R-project.org, version 4.0.3) or GraphPad Prism (version 8.0) software.

Results

Patients and clinical characteristics

The clinical characteristics of all participants in the sequencing cohort are provided in Table 1. The HBV DNA level was significantly higher in ACLF non-survivors than in survivors. Laboratory indicators, including total bilirubin, white blood cell count (WBC) and INR, were significantly worse in ACLF non-survivors than in survivors. The frequencies of organ failure in ACLF non-survivors were much higher than those in survivors, among which coagulation failure and cerebral failure were significantly different. The COSSH-ACLF, COSSH-ACLF II, CLIF-C ACLF, model for end-stage liver disease (MELD) and MELD-Na scores for ACLF non-survivors were significantly higher than those for survivors (all $p < 0.001$). These results showed significantly different clinical characteristics between ACLF non-survivors and survivors.

The clinical characteristics of patients with HBV-ACLF enrolled in the sequencing cohort and ELISA cohort were similar to those of the complete COSSH study open cohort (January 2015 to December 2020), which are summarized in Table S1. The proportions of ACLF-1, ACLF-2 and ACLF-3 were 57.6%, 36.2% and 6.2% in the complete COSSH study cohort, 58.6%, 35.7% and 5.7% in the sequencing cohort, and 72.2%, 22.7% and 5.1% in the ELISA cohort, which conforms with the development of epidemiological characteristics. The median hospital stay was 18.0 [9.0, 28.0] days in the complete COSSH study cohort, 17.5 [10.0, 24.7] days in the sequencing cohort and 18.0 [11.0, 25.0] days in the ELISA cohort. Of the 417 patients (417/1,895, 22.0%) who died in the intensive care unit (ICU) in the complete COSSH study cohort, 21 patients (21/70, 30.0%) died in the ICU in the sequencing cohort, and 49 patients (49/176, 27.8%) died in the ICU in the ELISA cohort. Patients who underwent liver transplantation were not enrolled in the current study to prevent the introduction of possible confounders.

Transcriptomic profiling of ACLF non-survivors

We performed mRNA sequencing analysis of patients with HBV-ACLF and different short-term outcomes, as well as controls. The two-dimensional PCA plot based on PC1 and PC2 revealed that the ACLF group had distinctive gene expression from the other control groups, and ACLF non-survivors deviated further from the control groups relative to survivors (Fig. S1). The pairwise differential expression analysis showed that compared to the healthy and CLD groups, ACLF survivors had 7,488 and 7,067 differentially expressed genes (DEGs), respectively, whereas these numbers were increased when the ACLF non-survivor group was compared to the healthy (8,312 DEGs) and CLD (7,391 DEGs) groups (Fig. S2). These results indicated a more disrupted transcriptomic profile in ACLF non-survivors than in survivors, which was consistent with the clinical characteristics of patients with multiple organ failures.

To further identify the biological pathways that are altered in parallel with disease progression, pairwise functional analysis between ACLF non-survivors and survivors based on GSEA was performed. The results showed that upregulation of gene sets related to metabolic pathways, such as "aerobic respiration", "2 oxoglutarate metabolic process" and "regulation of NADPH oxidase activity" and a downregulation of gene sets related to immune pathways, including "thymic T-cell selection", "cell proliferation in bone marrow" and "T-cell differentiation in thymus" were observed in ACLF non-survivors compared to survivors (Fig. 1B). These results suggested that the altered immune and metabolic bioprocesses were linked to the poor outcomes of patients with HBV-ACLF.

Immune cell alterations in ACLF

As the immune response changed during clinical deterioration, we further investigated changes in immune cell profiles. The immune cell types and their proportions were estimated based on transcriptomics by cellular deconvolution analysis using CIBERSORTx. The results showed that monocytes and lymphocytes were the main components of the PBMC samples (Fig. 2A). The proportion of monocytes gradually increased with disease progression, and there were significant differences between

Table 1. Clinical characteristics of patients in the sequencing group.

Characteristic	All HBV-ACLF (n = 70)	Non-survivor[#] (n = 24)	Survivor[#] (n = 46)	CLD (n = 20)	Healthy (n = 15)
Age (yrs.)	49 ± 10	50 ± 9	48 ± 11	45 ± 7	43 ± 10
Male (No.)	88.6% (62)	83.3% (20)	91.3% (42)	80.0% (16)	80.0% (12)
Complications					
GIH	4.3% (3)	8.3% (2)	2.2% (1)	0	0
Ascites	71.4% (50)	75.0% (18)	69.6% (32)	0	0
HE	20.0% (14)	41.7% (10)	8.7% (4)**	0	0
BI	28.6% (20)	37.5% (9)	23.9% (11)	0	0
HBV-DNA level (IU/ml)					
$\leq 2 \times 10^2$	11.4% (8)	12.5% (3)	10.9% (5)	90.0% (18)	n.a.
2×10^2 - 2×10^6	65.7% (46)	62.5% (15)	67.4% (31)	20.0% (2)	n.a.
$>2 \times 10^6$	22.9% (16)	25.0% (6)	21.7% (10)	0	n.a.
Laboratory data					
ALT (U/L)	222.0 [104.2, 484.5]	346.5 [130.7, 545.2]	164.5 [95.7, 346.5]	24.0 [21.0, 29.0]	21.8 ± 7.2
AST (U/L)	123.5 [82.7, 202.5]	128.5 [98.7, 221.0]	123.5 [79.0, 186.7]	24.0 [22.0, 25.0]	20.0 [13.0, 28.5]
Alb (g/L)	31.2 [28.7, 34.0]	31.5 ± 4.0	31.4 ± 3.6	48.1 ± 3.0	47.9 ± 3.1
ALP (U/L)	135.0 [110.5, 169.2]	131.0 [106.0, 173.0]	135.5 [115.2, 165.7]	80.0 ± 27.5	66.3 ± 22.1
TB (μmol/l)	347.0 [285.5, 426.5]	424.6 [347.8, 529.1]	326.5 [269.1, 401.2]***	16.0 [12.0, 20.0]	10.5 ± 2.9
Cr (μmol/L)	61.5 [53.0, 76.0]	61.0 [54.2, 77.7]	62.0 [53.0, 72.7]	73.1± 17.4	80.8 ± 11.1
Serum urea (mmol/L)	3.9 [2.9, 5.1]	4.8 [3.5, 6.0]	3.7 [2.8, 5.0]*	5.2 ± 1.5	5.0 ± 1.0
TG (mmol/L)	1.2 [1.0, 1.6]	1.1 ± 0.3	1.4 ± 0.4*	1.1 ± 0.7	1.9 ± 1.3
Tch (mmol/L)	2.1 [1.8, 2.4]	2.0 [1.5, 2.3]	2.2 [1.8, 2.4]	3.8 ± 0.7	4.6 ± 0.6
HDL-C (mmol/L)	0.2 [0.2, 0.3]	0.2 [0.2, 0.3]	0.2 [0.1, 0.3]	1.2 ± 0.2	1.2 ± 0.3
Na^+ (mmol/L)	138.0 [136.0, 140.0]	137.5 [135.0, 139.0]	138.5 [136.0, 140.0]	141.8 ± 2.1	142.1±2.5
WBC (10^9/L)	7.7 [5.7, 9.2]	8.7 [6.9, 10.5]	6.5 [4.8, 8.6]*	5.5 ± 1.3	6.30 ± 0.9
Monocytes (10^9/L)	0.8 [0.5, 1.0]	0.8 [0.7, 1.0]	0.6 [0.5, 0.9]	0.3 ± 0.1	0.33 ± 0.1
Neutrophils (10^9/L)	5.0 [3.4, 6.9]	6.5 [4.8, 8.0]	4.4 [2.9, 5.7]**	3.3 ± 1.1	3.91 ± 0.7
Lymphocytes (10^9/L)	1.2 [0.9, 1.5]	1.0 [0.8, 1.3]	1.2 [1.0, 1.8]*	1.7 ± 0.4	1.95 ± 0.5
NLR	3.9 [2.6, 6.9]	6.3 [4.0, 9.0]	3.0 [2.4, 4.9]**	2.0 ± 1.0	2.15 ± 0.8
hs-CRP (mg/L)	10.5 [6.2, 16.0]	7.7 [5.2, 12.3]	12.8 [8.2, 16.9]*	n.a.	n.a.
Hemoglobin (g/L)	123.0 [110.0, 136.0]	123.7 ± 20.8	123.1 ± 19.1	153.2 ± 11.9	149.6 ± 12.9
Hematocrit (%)	34.2 [30.5, 38.0]	34.3 [30.6, 38.0]	34.2 [30.6, 38.0]	44.8 ± 3.1	44.6 ± 3.6
PLT (10^9/L)	92.0 [69.2, 136.7]	85.5 [67.7, 100.7]	95.5 [74.5, 143.2]	150.0 [122.0, 183.0]	224.7 ± 41.5
INR	2.1 [1.9, 2.6]	2.7 [2.3, 3.2]	1.9 [1.7, 2.2]***	1.0 ± 0.1	n.a.
Fib (g/L)	1.3 [1.0, 1.6]	1.1 [0.8, 1.4]	1.4 [1.1, 1.7]**	n.a.	n.a.
PT (s)	23.9 [20.6, 27.7]	28.2 [25.0, 35.3]	22.0 [19.7, 24.2]***	n.a.	n.a.
AFP (ng/ml)	117.7 [44.4, 256.7]	60.9 [25.5, 245.8]	155.9 [64.9, 298.6]	2.4 ± 0.7	3.2 ± 2.0
Organ failure (No.)					
Liver	100.0% (70)	100.0% (24)	100.0% (46)	0	0
Coagulation	34.3% (24)	62.5% (15)	19.6% (9)**	0	0
Kidney	2.9% (2)	4.2% (1)	2.2% (1)	0	0
Cerebral	7.1% (5)	20.8% (5)	0.0% (0) **	0	0
Lung	0.0% (0)	0.0% (0)	0.0% (0)	0	0
Circulation	1.4% (1)	4.2% (1)	0.0% (0)	0	0
ACLF grade ***					
1	58.6% (41)	25.0% (6)	76.1% (35)	0	0
2	35.7% (25)	58.3% (14)	23.9% (11)	0	0
3	5.7% (4)	16.7% (4)	0.0% (0)	0	0
Severity score					
COSSH-ACLF	6.4 [5.7, 7.2]	7.3 [6.8, 8.0]	6.0 [5.5, 6.4]***	n.a.	n.a.
COSSH-ACLF II	7.3 [6.6, 8.0]	8.2 ± 0.8	6.9 ± 0.7***	n.a.	n.a.
CLIF-C ACLF	43.0 [38.3, 50.1]	49.0 ± 6.3	41.5 ± 5.7***	n.a.	n.a.
MELD	23.9 [20.8, 26.5]	26.5 [24.7, 29.6]	21.9 [19.8, 24.4]***	n.a.	n.a.
MELD-Na	24.8 [21.4, 27.5]	28.4 ± 4.7	23.2 ± 4.1***	n.a.	n.a.
Hospital stay (days)	17.5 [10.0, 24.7]	8.5 [3.7, 18.2]	23.0 [15.0, 33.7] ***	n.a.	n.a.
Died in ICU	30.0% (21)	75.0% (18)	6.5% (3) ***	n.a.	n.a.

ACLF, acute-on-chronic liver failure; AFP, alpha fetoprotein; Alb, albumin; ALP, alkaline phosphatase; ALT, alanine aminotransferase; AST, aspartate aminotransferase; BI, bacterial infection; CLD, chronic liver disease; COSSH-ACLF, Chinese Group on the Study of Severe Hepatitis B-ACLF; CLIF-C ACLF, Chronic Liver Failure- Consortium ACLF; Cr, creatinine; Fib, fibrinogen; GIH, gastrointestinal hemorrhage; HDL-C, high-density lipoprotein cholesterol; HE, hepatic encephalopathy; hs-CRP, high-sensitivity C-reactive protein; INR, international normalized ratio; MELD(-Na), model for end-stage liver disease(-sodium); NLR, neutrophil-to-lymphocyte ratio; PLT, platelet count; PT, prothrombin time; TB, total bilirubin; Tch, total cholesterol; TG, triglycerides; WBC, white blood cell count. NOTE. Data are expressed as the mean ± SD, median [Q1–Q3] or percentage (number of patients). Student's *t* test was used to compare continuous variables that were normally distributed. The Mann–Whitney *U* test was used to compare variables that were nonnormally distributed. Fisher's exact test was used to compare categorical variables.
*p <0.05, **p <0.01 and ***p value <0.001 for comparisons between nonsurvivor and survivor groups.
[#] Non-survivor, HBV-ACLF patients who died within 28 days; survivor, HBV-ACLF patients who survived within 28 days.

ACLF non-survivors and survivors (Fig. 2B). Macrophages, as a small proportion, were significantly higher in the ACLF group, including non-survivors and survivors, than in the other control groups (Fig. 2B). The proportions of NK cells and CD8+ T cells were significantly decreased in ACLF non-survivors (Fig. 2B). Survival analysis showed that patients with a comparatively high proportion of monocytes had a significantly higher mortality rate than patients with a low proportion (log-rank test p = 0.002),

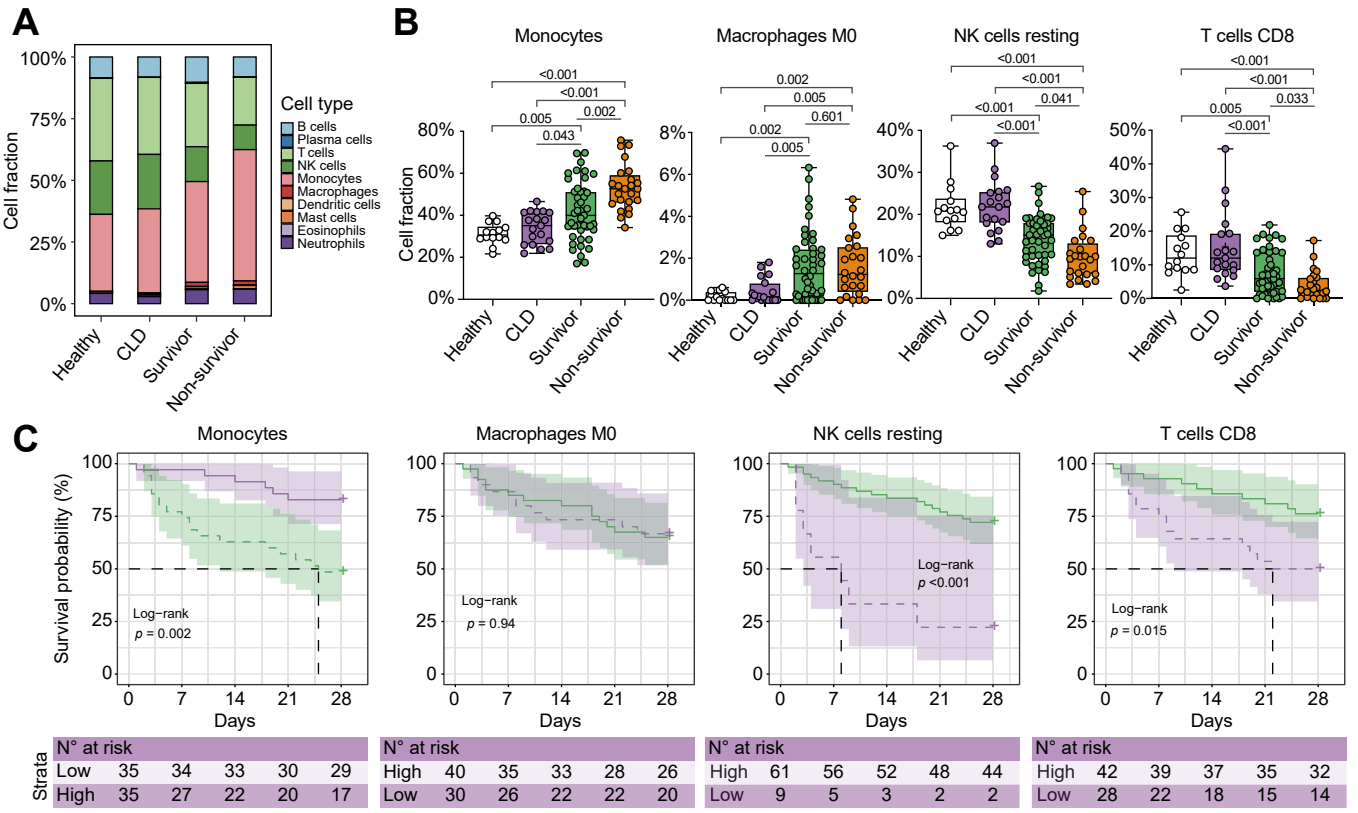

Fig. 2. Immune cell analysis related to poor ACLF outcomes. (A) CIBERSORTx cellular composition analysis predicting the proportion of 10 major immune cell types based on the transcriptome data of each patient, color-coded by cell type. (B) Changes in the proportions of immune cell types with ACLF progression. Level of significance: $p < 0.05$ (Kruskal–Wallis test). (C) Kaplan–Meier curves of survival probability stratified by the relative proportion of monocytes, M0 macrophages, resting NK cells, and CD8 T cells. The cut-off value of each immune cell was as follows: monocytes, 46.0%; macrophage M0, 1.0%; resting NK cells, 6.0%; CD8 T cells, 3%. Level of significance: $p < 0.05$ (log-rank test). ACLF, acute-on-chronic liver failure; CLD, chronic liver disease; NK, natural killer.

while patients with a comparatively low proportion of resting NK cells and CD8+ T cells had a higher mortality rate than patients with a high proportion (log-rank test $p < 0.001$ and $p = 0.015$, respectively) (Fig. 2C). These results showed that immune cell proportions were significantly correlated with poor ACLF outcomes.

Metabolic dysregulation related to ACLF mortality

Since altered metabolic pathways have been observed in ACLF non-survivors (Fig. 1B), we further investigated the metabolic reprogramming that underlies poor ACLF outcomes. Genes assigned to metabolic pathways from the KEGG database were extracted for analysis. PCA based on metabolic genes showed that the metabolic characteristics of ACLF non-survivors were different from those of survivors and controls (Fig. S3). The results of Euclidean distance based on metabolic expression profiles showed that the expression distance between ACLF non-survivors and survivors or controls was larger than the distance between ACLF survivors and controls or within controls (Fig. S4). The GSVA results showed that some lipid metabolic pathways were significantly altered when ACLF developed in the CLD or healthy groups, and four main metabolic category pathways (carbohydrates, energy, amino acids and xenobiotics) were more disrupted in the ACLF non-survivors than in survivors (Fig. 3A). Carbohydrate metabolism (the citrate cycle (TCA cycle), glycolysis/gluconeogenesis, the pentose phosphate pathway and pyruvate metabolism), energy metabolism (oxidative phosphorylation and sulfur metabolism) and amino acids (tryptophan metabolism) were significantly upregulated in ACLF non-survivors (all $p < 0.05$) (Fig. 3B).

VSIG4 is associated with ACLF mortality

Next, we searched for the key molecules related to short-term outcomes in ACLF. Differential expression analysis identified the top 10 candidate genes (*RNASE1, VSIG4, TMIGD3, ALOX15B, DAAM2, OLAH, CCL24, RLN3, AMPH, TIMP4*) that were significantly upregulated in ACLF non-survivors (Fig. 4A). Orthogonal partial least-squares discrimination analysis with variable importance in the projection (VIPpred) of the top 10 DEGs showed their discriminative capacity between ACLF non-survivors and survivors in the sequencing cohort (Fig. S5). The ROC analysis further confirmed their discriminative accuracy (Fig. S6). Based on the above results with a significance cut-off ($|\log_2$ fold change$| > 2$, adjusted $p < 0.05$, VIPpred >1 and AUROC >0.85), *VSIG4* was identified as the most robust predictor of survival in patients with ACLF ($\log_2$ fold change = 3.54, adjusted p value = 1.74×10^{-16}; VIPpred = 1.21; AUROC = 0.89) (Fig. 4A, Figs. S5-6). The mRNA expression levels of *VSIG4* were low in the CLD and healthy groups and were significantly upregulated in non-survivors (Fig. 4B), suggesting that *VSIG4* was a good prognostic biomarker.

We also dissected the pathways associated with *VSIG4* mRNA expression levels to investigate *VSIG4* biology. GSEA based on the

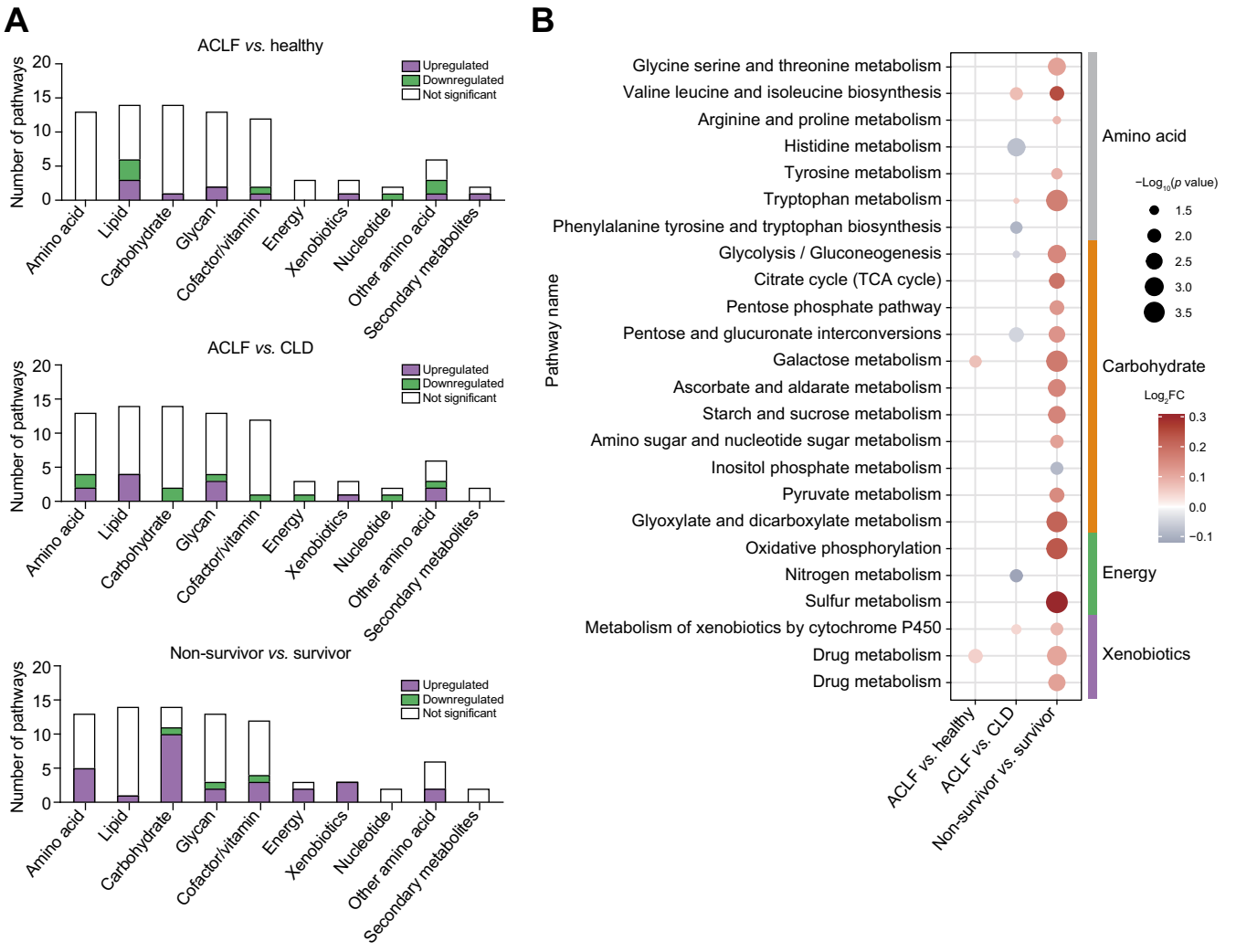

Fig. 3. Metabolic dysregulation related to poor ACLF outcomes. (A) The number of metabolic pathways that were significantly upregulated or downregulated (p value <0.05) in the comparisons of the ACLF non-survivor and survivor groups, ACLF and CLD groups, and ACLF and healthy groups among each of the 10 metabolic categories. (B) The significantly altered metabolic pathways identified in the comparisons of the ACLF non-survivor and survivor groups, ACLF and CLD groups, and ACLF and healthy groups among amino acid, carbohydrate, energy and xenobiotics metabolic categories (p value <0.05). ACLF, acute-on-chronic liver failure; CLD, chronic liver disease.

ordered gene list ranked by the value of Pearson's correlation coefficient with *VSIG4* expression was performed. The results showed that *VSIG4* levels were significantly positively correlated with multiple pathways involved in the development and progression of ACLF, including inflammation, enriched in monocytes, oxidative phosphorylation, the citrate cycle (TCA cycle), and glycolysis/gluconeogenesis (Fig. 4C). In addition, *VSIG4* levels were negatively correlated with gene sets related to T-cell differentiation/activation and enriched in NK cells (Fig. 4C). Consistently, the Pearson correlation analysis between the single-sample enrichment scores of each pathway and *VSIG4* mRNA expression levels showed a correlation with the inflammatory response, oxidative phosphorylation and T-cell selection/activation (Fig. S7). *VSIG4* mRNA levels were significantly associated with the fractions of monocytes, NK cells and CD8+ T cells (Fig. S8). These results suggested a correlation between *VSIG4* and immune-metabolism disorder in ACLF progression.

VSIG4 as a diagnostic biomarker for ACLF

We validated the *VSIG4* expression level by qRT−PCR in the same samples used for the sequencing cohort. The results showed that there were significant differences in *VSIG4* expression levels between the healthy/CLD and ACLF groups (Fig. 5A). The *VSIG4* expression level was significantly increased in ACLF non-survivors compared to survivors (p < 0.0001) (Fig. 5A). These data confirmed the reliability of the transcriptomic analysis results.

Next, for the convenience of clinical translation of the findings, we further investigated the relationship between plasma VSIG4 levels and ACLF progression by using ELISA in another cohort (Table S2). The results showed that plasma VSIG4 levels were significantly higher in the ACLF groups than in the CLD and healthy groups (p < 0.0001) (Fig. 5B), and the AUROC of VSIG4 levels for the differentiation of ACLF from the CLD and healthy groups was 0.983 (Fig. 5C). These results showed that VSIG4 was

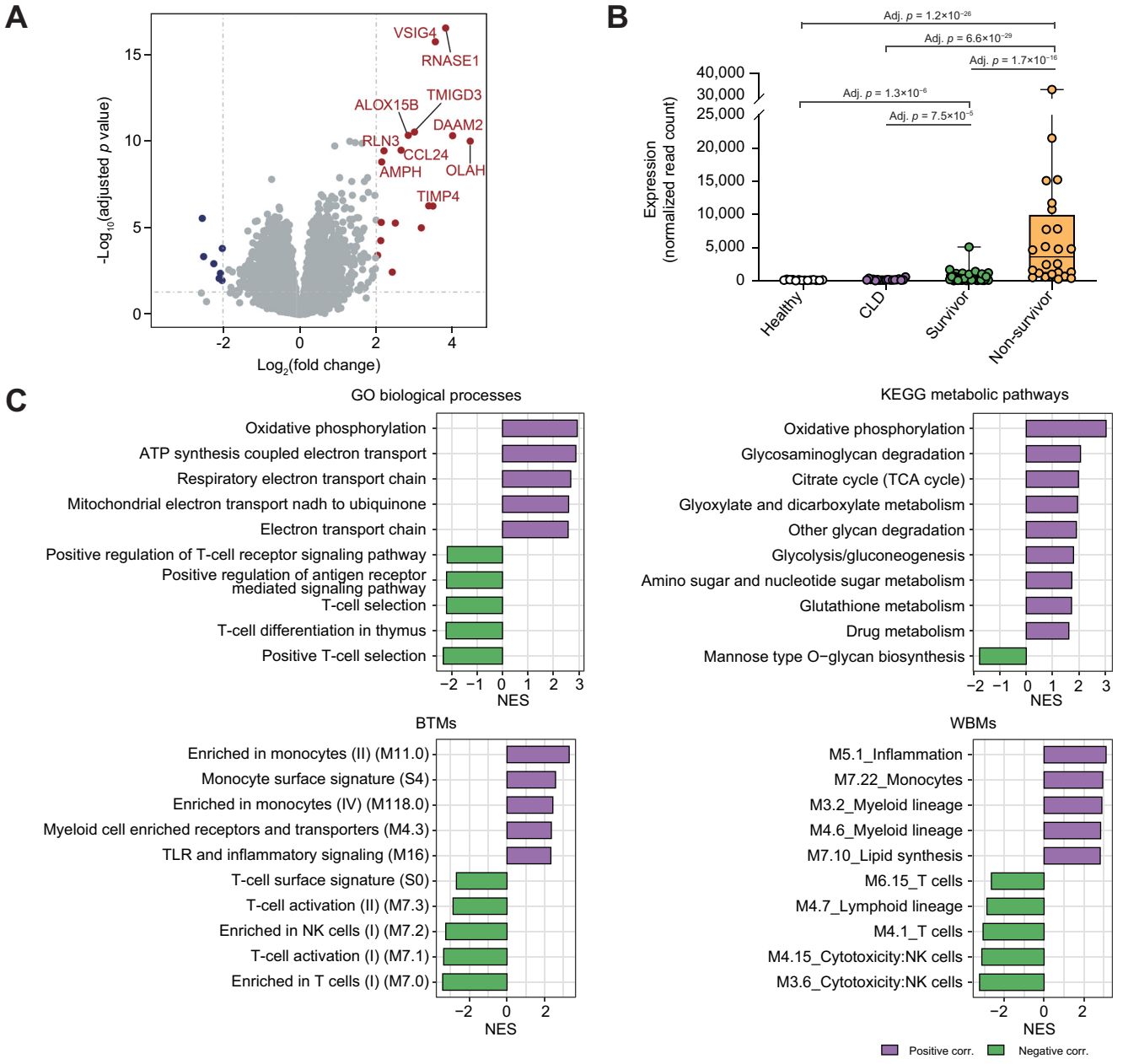

Fig. 4. Peripheral blood mononuclear cell transcriptomic profiling identifying the *VSIG4* expression level as strongly associated with poor ACLF outcomes. (A) Volcano plot depicting DEGs between ACLF non-survivors and survivors in the sequencing derivation cohort. Significant DEGs (|log2 fold change| >2; adjusted *p* value <0.05) are shown in red or blue. (B) Boxplots showing *VSIG4* mRNA expression levels in the ACLF non-survivor, survivor, CLD and healthy groups. Level of significance: adj $p < 0.05$ (Wald test and corrected by Benjamini–Hochberg procedure). (C) Gene set-enrichment analysis results based on the rank-ordered gene list according to the Pearson's correlation coefficient with *VSIG4* mRNA level. The top 10 significantly enriched gene ontology biological processes are shown in each plot. ACLF, acute-on-chronic liver failure; BTMs, blood transcriptional modules; DEGs, differentially expressed genes; GO, gene ontology; NES, normalized enrichment score; NK, natural killer; WBMs, whole blood modules.

a good diagnostic marker for distinguishing between ACLF and stable disease status. Moreover, the plasma VSIG4 level was significantly higher in ACLF non-survivors than in survivors ($p = 0.0001$) (Fig. 5B). The VSIG4 expression level was also significantly increased with ACLF grade (Fig. 5D). There were significant differences in VSIG4 levels between patients with and without coagulation failure, cerebral failure and kidney failure (Fig. 5E, $p = 0.0002/0.005/0.010$). The plasma VSIG4 level was significantly associated with key indicators and clinical scores, including positive correlations with WBC ($R = 0.33$, $p < 0.001$), INR ($R = 0.4$, $p < 0.001$), neutrophils ($R = 0.41$, $p < 0.001$), urea ($R = 0.65$, $p < 0.001$), COSSH-ACLF II score ($R = 0.71$, $p < 0.001$) and CLIF-C ACLF score ($R = 0.59$, $p < 0.001$) (Fig. S9). These results suggested that VSIG4, as a diagnostic biomarker for ACLF, could reflect inflammation, coagulation status and disease severity.

Prognostic performance of VSIG4

Next, we investigated the potential of VSIG4 as a non-invasive plasma biomarker to distinguish non-survivors from survivors. ROC analysis showed that the prognostic accuracy of plasma

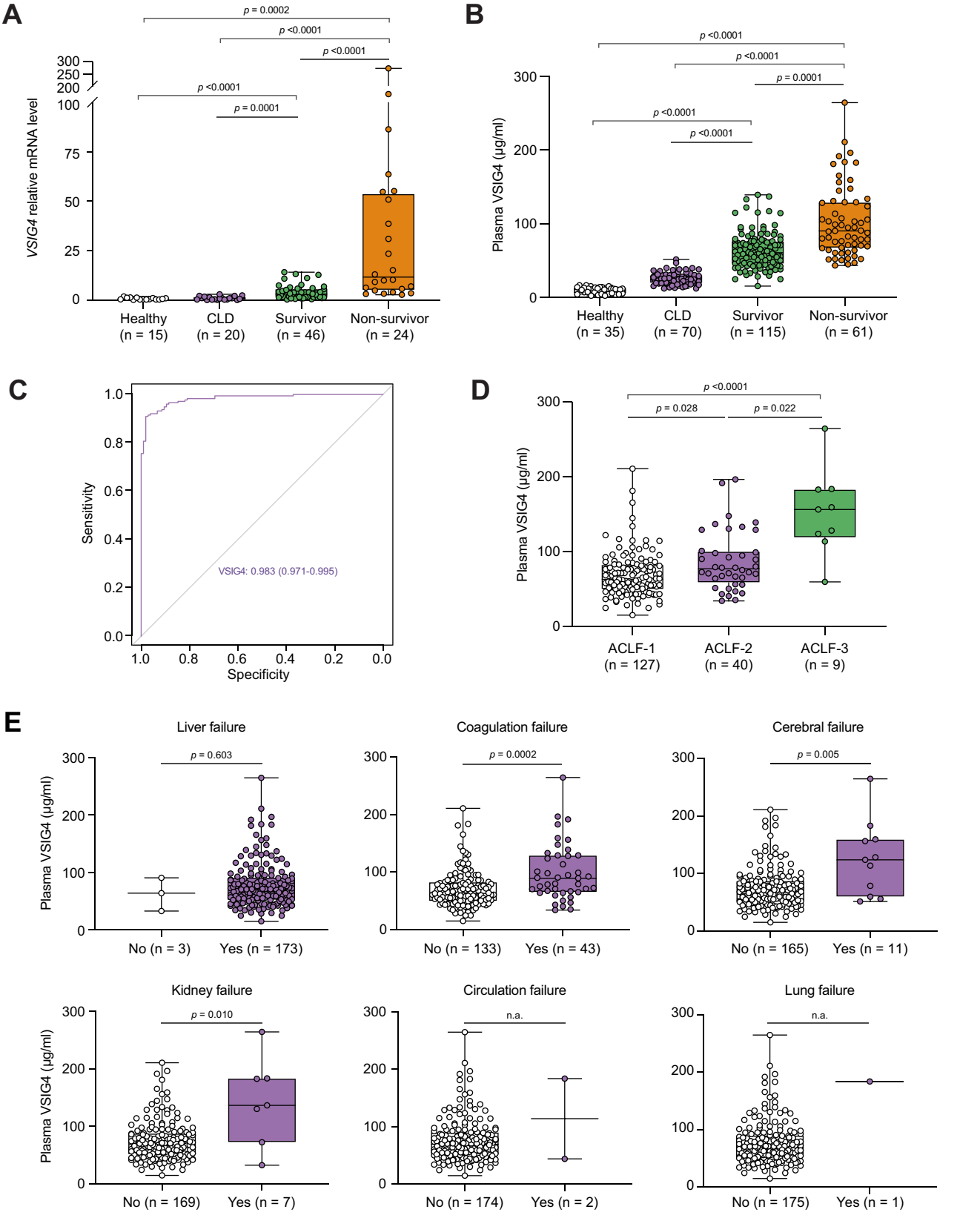

Fig. 5. Validation of VSIG4 expression levels in ACLF. (A) Peripheral blood mononuclear cell *VSIG4* expression levels were tested by qRT–PCR in the same patients analyzed for the sequencing cohort. Level of significance: $p < 0.05$ (Kruskal–Wallis test. ANOVA). (B) Plasma VSIG4 expression levels in patients at different disease stages tested by ELISA. Level of significance: $p < 0.05$ (Kruskal–Wallis test. ANOVA). (C) ROC curves of plasma VSIG4 expression levels for distinguishing patients with ACLF from those with CLD and healthy controls. (D) Boxplots showing plasma VSIG4 expression levels stratified by ACLF grade. Level of significance: $p < 0.05$ (Kruskal–Wallis test. ANOVA) (E) Boxplots showing plasma VSIG4 expression levels stratified by the presence of organ failure. Level of significance: $p < 0.05$ (Mann–Whitney test). ACLF, acute-on-chronic liver failure; CLD, chronic liver disease; qRT-PCR, quantitative reverse-transcription PCR.

VSIG4 levels for predicting 28-/90-day mortality was 0.769/0.767, which was comparable to that of three commonly used clinical scores (COSSH-ACLF, AUROC = 0.867/0.884, p = 0.014/0.002; CLIF-C ACLF, AUROC = 0.840/0.835, p = 0.070/0.058; MELD-Na, AUROC = 0.710/0.737, p = 0.217/0.509) (Fig. 6A). In the multivariate analysis, the association of VSIG4 with ACLF outcomes was independent of clinical scores (Fig. 6B). VSIG4 evaluation improved the prognostic performance of the COSSH-ACLF score for 28-/90-day mortality (AUROC, 28-day: 0.890 *vs.* 0.867, p = 0.063; 90-day: 0.899 *vs.* 0.884, p = 0.162), CLIF-C ACLF score (AUROC, 28-day: 0.855 *vs.* 0.840, p = 0.066; 90-day: 0.854 *vs.* 0.835, p = 0.034) and MELD-Na score (AUROC, 28-day: 0.789 *vs.* 0.710, p = 0.047; 90-day: 0.796 *vs.* 0.737, p = 0.091) (Fig. 6A and B). These results showed the high specificity of VSIG4 for identifying ACLF non-survivors.

Risk stratification of plasma VSIG4 levels

For the convenience of clinical application, risk stratification by plasma VSIG4 expression levels was conducted using X-tile plots. The patients were separated into two groups with highly different probabilities of survival according to the optimal cut-off value of the plasma VSIG4 level: low-risk group (plasma VSIG4 level <122 μg/ml, n = 155) and high-risk group (plasma VSIG4 level ≥122 μg/ml, n = 21). The clinical characteristics of patients in the low-risk group and high-risk group are provided in Table S3. The laboratory indicators, including creatinine, serum urea, neutrophil count, lymphocyte count and INR, were significantly worse in the high-risk group than in the low-risk group. The patients in the high-risk group exhibited more frequent complications than those in the low-risk group (gastrointestinal hemorrhage, 47.6%/7.7%, p < 0.001; ascites, 19.0%/3.2%, p = 0.010; hepatic encephalopathy, 85.7%/63.9%, p = 0.081; bacterial infection, 47.6%/25.8%, p = 0.068). The frequencies of organ failure in the high-risk group were much higher than those in the low-risk group, among which coagulation failure, kidney failure and cerebral failure were significantly different. The COSSH-ACLF, COSSH-ACLF II, CLIF-C ACLF, MELD and MELD-Na scores for patients in the high-risk group were significantly higher than those for patients in the low-risk group (all p < 0.001). Notably, all 21 patients (21/21, 100%) with high plasma VSIG4 levels died before 45 days. Kaplan–Meier survival analysis showed a significant difference between the low-risk and high-risk groups (p < 0.0001 at 28/90 days) (Fig. 6C).

Generality of VSIG4 in ACLF

We next evaluated plasma VSIG4 levels in patients with non-HBV-ACLF. The clinical characteristics of these patients are provided in Table S4. Plasma VSIG4 levels were also significantly different between non-HBV-ACLF non-survivors and survivors (p = 0.0017) (Fig. 7A). VSIG4 expression gradually increased with ACLF grade and was significantly associated with coagulation failure and lung failure (Fig. 7A and Fig. S10, p = 0.066/0.048/0.016). The plasma VSIG4 levels were negatively correlated with C-reactive protein (R = -0.48, p = 0.012) and positively correlated with age (R = 0.51, p < 0.001), alkaline phosphatase (R = 0.42, p = 0.0077), creatinine (R = 0.4, p = 0.011), serum urea (R = 0.41, p = 0.0082), CLIF-C ACLF (R = 0.54, p < 0.001), COSSH-ACLF II (R = 0.55, p < 0.001), and MELD (R = 0.37, p = 0.019) scores (Fig. S11). ROC analysis showed that the prognostic accuracy of plasma VSIG4 levels for predicting 28-/90-day mortality was 0.813/0.776 in patients with non-HBV-ACLF, which was comparable to that of three commonly used clinical scores (*e.g.* COSSH-ACLF, AUROC = 0.859/0.813, p = 0.659/0.729; CLIF-C ACLF, AUROC = 0.818/0.854, p = 0.951/0.374; MELD-Na, AUROC = 0.665/0.627, p = 0.162/0.182) (Fig. 7B). Kaplan–Meier survival analysis showed a significant difference between the low-risk (plasma VSIG4 level <122 μg/ml, n = 24) and high-risk (plasma VSIG4 level ≥122 μg/ml, n = 16) groups of patients with non-HBV-ACLF (p < 0.0001/=0.0081 at 28/90 days) (Fig. 7C). These results suggested that plasma VSIG4 levels may be a good predictor of mortality risk in patients with ACLF, regardless of etiology.

Discussion

HBV-ACLF exhibits different clinical characteristics from alcohol-related ACLF. Elucidating the pathophysiological characteristics underlying short-term outcomes and identifying prognostic biomarkers of HBV-ACLF could help to reduce its high mortality. In this study, we performed systematic analyses based on transcriptomics with PBMCs and found significantly altered molecular characteristics in patients with HBV-ACLF and different outcomes. Moreover, we identified VSIG4 as an effective biomarker associated with ACLF mortality, which was further validated in an external cohort at the serological level.

Accumulating evidence has revealed that immune dysregulation and metabolic disorders play an important role during the progression of ACLF.[8,25,26] However, very few studies have focused on the molecular basis of different outcomes. Our previous works have reported that immune-metabolism disorder is a core axis of disease development in patients with ACLF.[8,27] EASL-CLIF reported that dysregulation of glycolysis and inhibition of mitochondrial energy production were correlated with ACLF.[25,28] In this study, we also observed that immune dysregulation was involved in poor ACLF outcomes, and a significant alteration in immune cells during disease progression was identified. Studies have reported that recruited monocytes are key drivers of the inflammatory phenotype and cytokine storm, which might contribute to ACLF disease severity.[29,30] The lower level of NK cells illustrated that the ability to clear virus-infected cells and release antiviral cytokines might be weakened in ACLF non-survivors.[31] Moreover, a more compromised adaptive immune system with T-cell exhaustion occurred in ACLF non-survivors. Patients with alcohol-related ACLF also exhibited disordered monocyte counts and decreased proportions of NK cells and CD8+ T cells.[32,33] These results revealed that disordered immune cells and perturbance of the immune response were associated with poor ACLF outcomes. Pathways involved in lipid, energy, and carbohydrate metabolism and glycan biosynthesis were more significantly altered in ACLF non-survivors. Glycolysis/gluconeogenesis and the pentose phosphate pathway were activated in patients with worse outcomes, which could support the metabolism required for cell growth and proliferation.[34] The TCA cycle is a highly efficient mode of ATP generation that can satisfy the high energy demand of activated immune cells.[35] We also found that sulfur metabolism, which is important in oxidative stress regulation and detoxification for recovery from liver damage, was correlated with ACLF mortality.[36] These results illustrated that metabolic reprogramming altered the immune cell response to cope with the pathophysiological changes that occur in ACLF. Peripheral immune cell changes and metabolic alterations in specific immune cell subpopulations need to be further analyzed at the single-cell level.

The identification of diagnostic and prognostic biomarkers associated with disease pathogenesis could be used to optimize

A

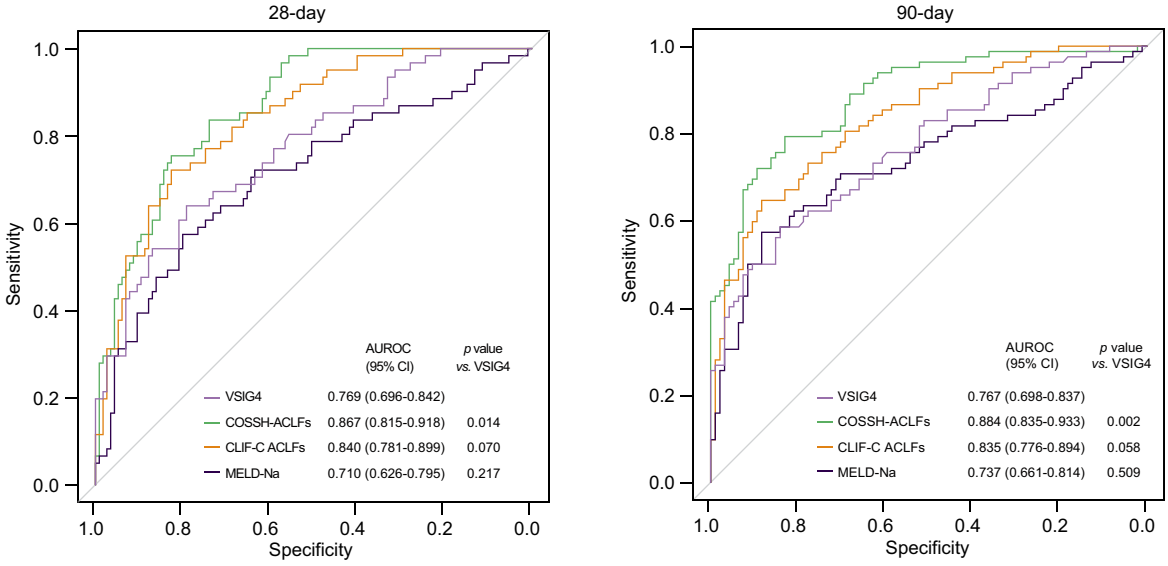

B

The prognostic score formulas according to multivariate COX PH model.

		Multivariate COX PH regression			ROC analysis			
		Coefficient	HR [95% CI]	*p* value[a]	AUROC of 28-day	*p* value[b]	AUROC of 90-day	*p* value[b]
COSSH-ACLFs+VSIG4	COSSH-ACLFs	0.75	2.12 [1.64, 2.74]	<0.001	0.890	0.063	0.899	0.162
	VSIG4	0.0079	1.01 [1.00, 1.02]	0.030				
CLIF-C ACLFs+VSIG4	CLIF-C ACLFs	0.12	1.12 [1.08, 1.17]	<0.001	0.855	0.066	0.854	0.034
	VSIG4	0.0092	1.01 [1.00, 1.02]	0.004				
MELD-Na+VSIG4	MELD-Na	0.047	1.05 [1.00, 1.10]	0.046	0.789	0.047	0.796	0.091
	VSIG4	0.016	1.02 [1.01, 1.02]	<0.001				

[a] The *p* value was calculated by the multivariate COX PH regression.
[b] The *p* value was from comparisons of AUROC between the new developed prognostic score and COSSH-ACLFs, CLIF-C ACLFs or MELD-Na.

C

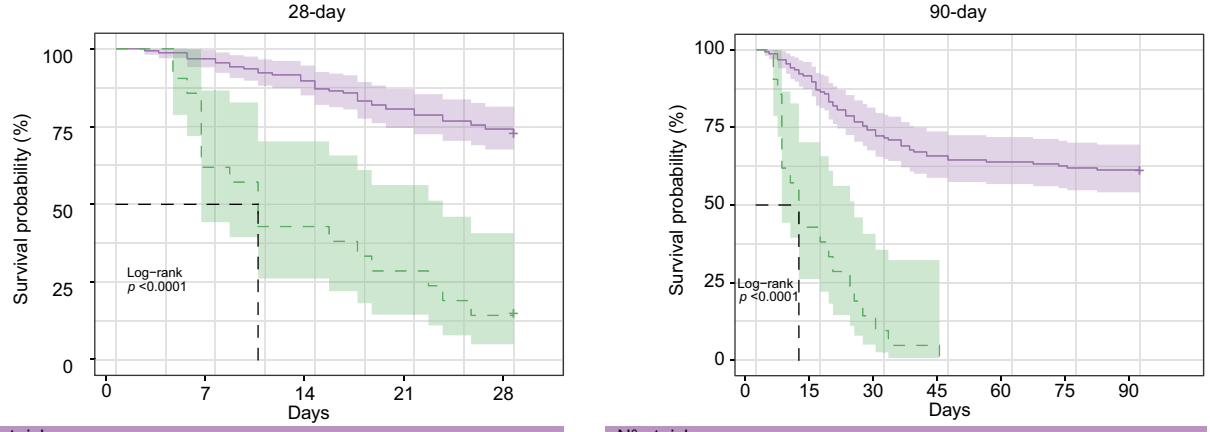

Fig. 6. Prognostic accuracy and risk stratification of plasma VSIG4 levels. (A) ROC curves of plasma VSIG4 expression levels for predicting the 28-day (left) and 90-day (right) mortality of patients with ACLF compared to three clinical scores. Level of significance: $p < 0.05$ (DeLong test). (B) The prognostic score formulas according to the multivariate Cox proportional hazards model. (C) Kaplan–Meier curves of survival probability stratified by plasma VSIG4 level at 28 days (left) and 90 days (right). Level of significance: $p < 0.05$ (log-rank test). The number of patients at risk is shown for each observation period. ACLF, acute-on-chronic liver failure; COSSH-ACLF, Chinese Group on the Study of Severe Hepatitis B-ACLF; CLIF-C ACLF, Chronic Liver Failure-Consortium ACLF; MELD-Na, model for end-stage liver disease-sodium; PH, proportional hazards.

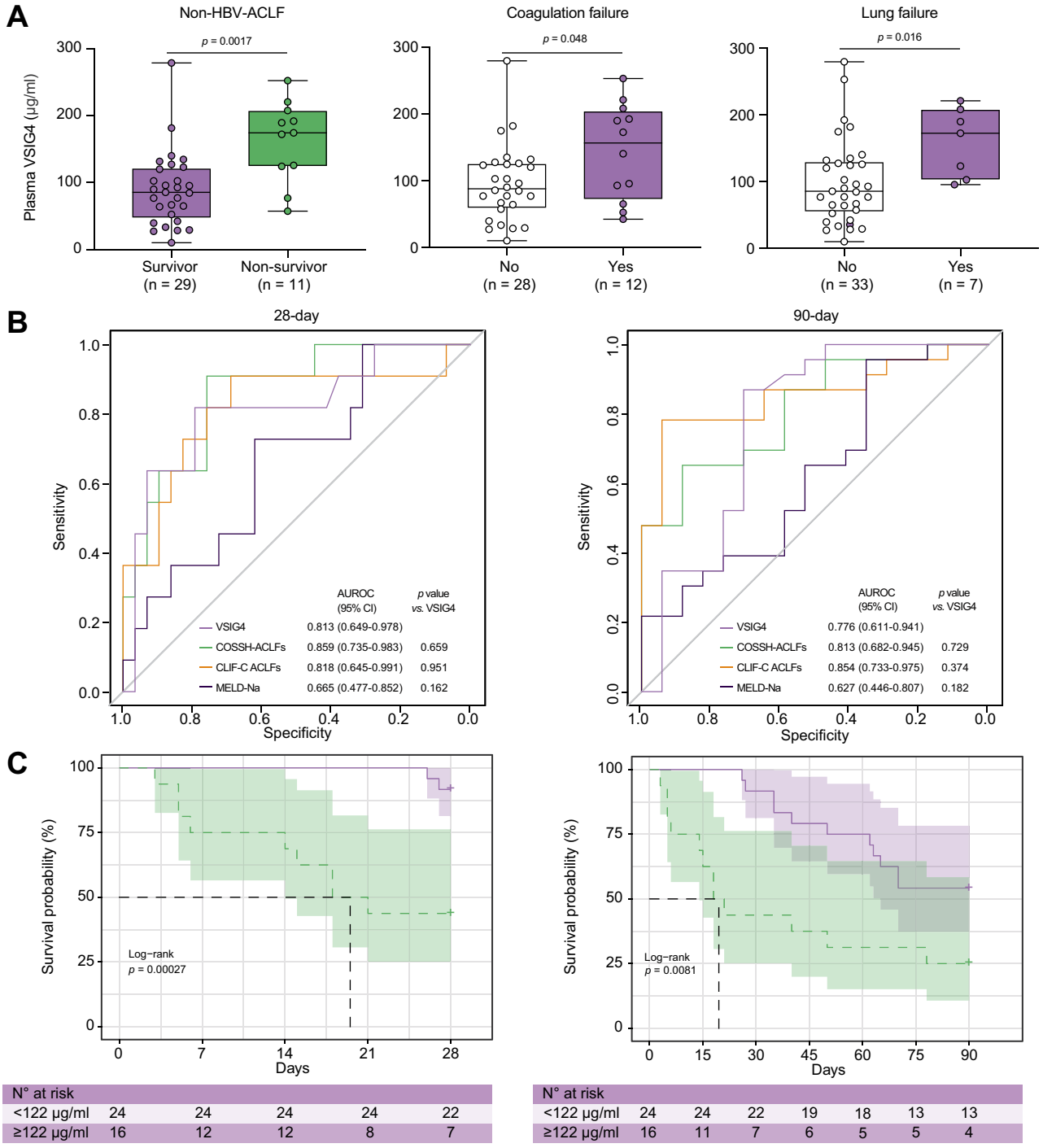

Fig. 7. Validation of VSIG4 expression levels in patients with non-HBV-ACLF. (A) Boxplots showing plasma VSIG4 expression levels stratified by non-HBV-ACLF outcomes at 28 days, and the presence of coagulation and lung failure. Level of significance: $p < 0.05$ (Mann–Whitney test). (B) ROC curves of plasma VSIG4 expression levels for predicting the 28-day (left) and 90-day (right) mortality of patients with non-HBV-ACLF compared to three clinical scores. Level of significance: $p < 0.05$ (DeLong test). (C) Kaplan–Meier curves of survival probability stratified by plasma VSIG4 level at 28 days (left) and 90 days (right). Level of significance: $p < 0.05$ (log-rank test). The number of patients at risk is shown for each observation period. ACLF, acute-on-chronic liver failure; COSSH-ACLF, Chinese Group on the Study of Severe Hepatitis B-ACLF; CLIF-C ACLF, Chronic Liver Failure-Consortium ACLF; MELD-Na, model for end-stage liver disease-sodium.

the prediction of clinical events in patients with ACLF. One prospective study revealed that urinary liver fatty acid-binding protein, which has been reported to be involved in lipid metabolism, may be a potential biomarker for predicting the prognosis of patients with decompensated cirrhosis. However, the role of urinary liver fatty acid-binding protein in the pathophysiology of ACLF has not been determined.[37] Another study found that the level of urine neutrophil gelatinase-associated lipocalin, which has been hypothesized to be correlated with liver failure and systemic inflammation, was markedly

upregulated in patients with ACLF and could be used to improve the prognostic accuracy together with the MELD score in patients with decompensated cirrhosis.[38] Despite extensive studies, biomarkers reflecting the molecular basis of ACLF and associated with the diagnosis and prognosis of ACLF remain limited. In the present study, based on transcriptomics data and ELISA data, VSIG4 was confirmed as a robust biomarker for predicting 28-/90-day mortality in patients with HBV-ACLF. As a single molecule, the performance of VSIG4 for predicting ACLF outcomes was comparable to that of commonly used clinical prognostic scores, including COSSH-ACLF, CLIF-C ACLF and MELD-Na. The optimal cut-off value of the plasma VSIG4 level was established to specifically identify patients with ACLF at high risk of death. This could be useful for monitoring the risk and progression of ACLF in clinical practice. VSIG4 has also been found to be significantly upregulated in patients with non-HBV-ACLF, suggesting its potential role in ACLF regardless of etiology.[32] Plasma VSIG4 levels in patients with different etiologies were also measured in our study and showed good accuracy for differentiating ACLF non-survivors from survivors. Due to the limited number of patients with other etiologies, the generalizability of VSIG4 requires further validation in other larger groups.

VSIG4, a macrophage complement receptor (also referred to as CRIg), is a critical component of the innate and adaptive immune systems.[39] It has been demonstrated to induce tolerance in T cells and NKT cells and protect against immune-mediated liver injury.[40] VSIG4 can inhibit macrophage-dependent inflammation by reprogramming mitochondrial pyruvate metabolism.[41] Higher peritoneal VSIG4 levels can be used to predict the prognosis of spontaneous bacterial peritonitis, while regulating the ratio of VSIG4-expressing macrophage subpopulations might provide new therapies for cirrhosis and ascites.[42,43] Our results showed that the *VSIG4* expression level was significantly correlated with T-cell activation/differentiation and inflammatory response-related bioprocesses and positively associated with WBC, INR and neutrophil levels in patients with HBV-ACLF, which is consistent with the findings of previous studies, indicating that the potential function of VSIG4 may be to correct immune disorders during ACLF progression. VSIG4 is tightly linked with serum urea levels, which might alleviate acute kidney injury by suppressing inflammation.[44] VSIG4 might be shed as a soluble protein to inhibit T-cell activation by suppressing complement activation.[45–47] In addition, the strong correlation between VSIG4 and COSSH-ACLF II score shows the good prognostic performance of VSIG4. The mechanisms underlying the role of VSIG4 in ACLF need to be clarified in future studies.

In summary, this study identified immune cell proportions as a critical factor associated with poor HBV-ACLF outcomes and revealed that disordered metabolic pathways meet the high energy demand of immune cells to regulate the immune response. We identified and validated VSIG4, which was correlated with the pathophysiological basis of ACLF, as a diagnostic and prognostic biomarker for ACLF. The findings of this study could be used to develop a simple and accurate method for diagnosing and determining the prognosis of patients with HBV-ACLF.

Abbreviations

ACLF, acute-on-chronic liver failure; CHB, chronic hepatitis B; CLD, chronic liver disease; COSSH, Chinese Group on the Study of Severe Hepatitis B; DEGs, differentially expressed genes; EASL-CLIF, European Association for the Study of the Liver-Chronic Liver Failure; GSEA, gene set enrichment analysis; GSVA, gene set variation analysis; INR, international normalized ratio; MELD(-Na), model for end-stage liver disease(-sodium); PBMCs, peripheral blood mononuclear cells; PCA, principal component analysis; qRT–PCR, quantitative reverse-transcription PCR; VIPpred, variable importance in the projection; VSIG4, V-set and immunoglobulin domain-containing 4; WBC, white blood cell.

Financial support

The National Natural Science Foundation of China (81830073, 81901901, 82272426), the National and Zhejiang Provincial special support program for high-level personnel recruitment (Ten-thousand Talents Program), the Zhejiang Public Welfare Project (LGF21H200006, LY21H030007), and National Key Research and Development Program of China (2022YFC2304800, 2022YFA1104100) provided financial support for the study.

Conflict of interest

The authors declare that they have no conflicts of interest.

Please refer to the accompanying ICMJE disclosure forms for further details.

Authors' contributions

XL, PL, JJ and JJX contributed equally. The study was designed by JL, DYS and XC. JL, DYS, XL and PL wrote the manuscript. XL, PL, JJ and CPC performed the statistical and bioinformatics analyses. PL, JJX, JJL, JQL, KKR, QZ, BBG, XPZ, JXC, LLH, HY, WH, SWM and BQL performed the laboratory work. All authors approved the final version of the manuscript.

Data available statement

All data relevant to the study have been included in the article or uploaded as supplementary information. The datasets for transcriptome sequencing are available in the Sequence Read Archive database (accession number: PRJNA548207). The added datasets for transcriptome sequencing are available on reasonable request from the corresponding author.

Ethics approval

The study protocol was approved by the Clinical Research Ethics Committee of the First Affiliated Hospital, Zhejiang University School of Medicine (No. 2016-31). All patients were well informed, and written consent was obtained from them or their legal surrogates before enrollment.

Acknowledgments

We would like to thank all the doctors and nurses in the COSSH open cohort study for their selfless dedication and help in completing the study.

Supplementary data

Supplementary data to this article can be found online at https://doi.org/10.1016/j.jhepr.2023.100848.

References

Author names in bold designate shared co-first authorship

[1] **Wu T**, **Li J**, **Shao L**, Xin J, Jiang L, Zhou Q, et al. Development of diagnostic criteria and a prognostic score for hepatitis B virus-related acute-on-chronic liver failure. Gut 2018;67:2181–2191.

[2] Arroyo V, Moreau R, Jalan R. Acute-on-Chronic liver failure. N Engl J Med 2020;382:2137–2145.
[3] **Luo J**, **Liang X**, **Xin J**, **Li J**, Li P, Zhou Q, et al. Predicting the onset of hepatitis B virus-related acute-on-chronic liver failure. Clin Gastroenterol Hepatol 2023;21(3):681–693.
[4] **Jalan R**, **Saliba F**, **Pavesi M**, Amoros A, Moreau R, Gines P, et al. Development and validation of a prognostic score to predict mortality in patients with acute-on-chronic liver failure. J Hepatol 2014;61:1038–1047.
[5] **Li J**, **Liang X**, **You S**, **Feng T**, **Zhou X**, **Zhu B**, et al. Development and validation of a new prognostic score for hepatitis B virus-related acute-on-chronic liver failure. J Hepatol 2021;75:1104–1115.
[6] **Claria J**, **Stauber RE**, Coenraad MJ, Moreau R, Jalan R, Pavesi M, et al. Systemic inflammation in decompensated cirrhosis: characterization and role in acute-on-chronic liver failure. Hepatology 2016;64:1249–1264.
[7] **Graupera I**, **Isus L**, Coll M, Pose E, Diaz A, Vallverdu J, et al. Molecular characterization of chronic liver disease dynamics: from liver fibrosis to acute-on-chronic liver failure. JHEP Rep 2022;4:100482.
[8] **Li J**, **Liang X**, **Jiang J**, **Yang L**, Xin J, Shi D, et al. PBMC transcriptomics identifies immune-metabolism disorder during the development of HBV-ACLF. Gut 2022;71:163–175.
[9] Sarin SK, Kumar A, Almeida JA, Chawla YK, Fan ST, Garg H, et al. Acute-on-chronic liver failure: consensus recommendations of the Asian Pacific Association for the study of the liver (APASL). Hepatol Int 2009;3:269–282.
[10] Moreau R, Jalan R, Gines P, Pavesi M, Angeli P, Cordoba J, et al. Acute-on-chronic liver failure is a distinct syndrome that develops in patients with acute decompensation of cirrhosis. Gastroenterology 2013;144:1426–1437. 1437 e1-9.
[11] Lok AS, McMahon BJ. Chronic hepatitis B: update 2009. Hepatology 2009;50:661–662.
[12] Brown J, Pirrung M, McCue LA. FQC Dashboard: integrates FastQC results into a web-based, interactive, and extensible FASTQ quality control tool. Bioinformatics 2017;33:3137–3139.
[13] Bolger AM, Lohse M, Usadel B. Trimmomatic: a flexible trimmer for Illumina sequence data. Bioinformatics 2014;30:2114–2120.
[14] Kim D, Landmead B, Salzberg SL. HISAT: a fast spliced aligner with low memory requirements. Nat Methods 2015;12. 357-U121.
[15] Anders S, Pyl PT, Huber W. HTSeq–a Python framework to work with high-throughput sequencing data. Bioinformatics 2015;31:166–169.
[16] Love MI, Huber W, Anders S. Moderated estimation of fold change and dispersion for RNA-seq data with DESeq2. Genome Biol 2014;15:550.
[17] Newman AM, Liu CL, Green MR, Gentles AJ, Feng W, Xu Y, et al. Robust enumeration of cell subsets from tissue expression profiles. Nat Methods 2015;12:453–457.
[18] Newman AM, Steen CB, Liu CL, Gentles AJ, Chaudhuri AA, Scherer F, et al. Determining cell type abundance and expression from bulk tissues with digital cytometry. Nat Biotechnol 2019;37:773–782.
[19] Hanzelmann S, Castelo R, Guinney J. GSVA: gene set variation analysis for microarray and RNA-seq data. BMC Bioinformatics 2013;14:7.
[20] Li S, Rouphael N, Duraisingham S, Romero-Steiner S, Presnell S, Davis C, et al. Molecular signatures of antibody responses derived from a systems biology study of five human vaccines. Nat Immunol 2014;15:195–204.
[21] Banchereau R, Hong S, Cantarel B, Baldwin N, Baisch J, Edens M, et al. Personalized immunomonitoring uncovers molecular networks that stratify lupus patients. Cell 2016;165:551–565.
[22] **Subramanian A**, **Tamayo P**, Mootha VK, Mukherjee S, Ebert BL, Gillette MA, et al. Gene set enrichment analysis: a knowledge-based approach for interpreting genome-wide expression profiles. Proc Natl Acad Sci U S A 2005;102:15545–15550.
[23] Liberzon A, Birger C, Thorvaldsdottir H, Ghandi M, Mesirov JP, Tamayo P. The Molecular Signatures Database (MSigDB) hallmark gene set collection. Cell Syst 2015;1:417–425.
[24] Camp RL, Dolled-Filhart M, Rimm DL. X-tile: a new bio-informatics tool for biomarker assessment and outcome-based cut-point optimization. Clin Cancer Res 2004;10:7252–7259.
[25] **Moreau R**, **Claria J**, **Aguilar F**, **Fenaille F**, Lozano JJ, Junot C, et al. Blood metabolomics uncovers inflammation-associated mitochondrial dysfunction as a potential mechanism underlying ACLF. J Hepatol 2020;72:688–701.
[26] Garg V, Garg H, Khan A, Trehanpati N, Kumar A, Sharma BC, et al. Granulocyte colony-stimulating factor mobilizes CD34(+) cells and improves survival of patients with acute-on-chronic liver failure. Gastroenterology 2012;142:505–512 e1.
[27] **Hassan HM**, **Cai Q**, **Liang X**, Xin J, Ren K, Jiang J, et al. Transcriptomics reveals immune-metabolism disorder in acute-on-chronic liver failure in rats. Life Sci Alliance 2022;5.
[28] Zhang IW, Curto A, Lopez-Vicario C, Casulleras M, Duran-Guell M, Flores-Costa R, et al. Mitochondrial dysfunction governs immunometabolism in leukocytes of patients with acute-on-chronic liver failure. J Hepatol 2022;76:93–106.
[29] Shi C, Pamer EG. Monocyte recruitment during infection and inflammation. Nat Rev Immunol 2011;11:762–774.
[30] **Vanderbeke L**, **Van Mol P**, **Van Herck Y**, **De Smet F**, **Humblet-Baron S**, **Martinod K**, et al. Monocyte-driven atypical cytokine storm and aberrant neutrophil activation as key mediators of COVID-19 disease severity. Nat Commun 2021;12:4117.
[31] Jegaskanda S, Vanderven HA, Tan HX, Alcantara S, Wragg KM, Parsons MS, et al. Influenza virus infection enhances antibody-mediated NK cell functions via type I interferon-dependent pathways. J Virol 2019;93.
[32] **Weiss E**, **de la Grange P**, Defaye M, Lozano JJ, Aguilar F, Hegde P, et al. Characterization of blood immune cells in patients with decompensated cirrhosis including ACLF. Front Immunol 2020;11:619039.
[33] Bernsmeier C, Pop OT, Singanayagam A, Triantafyllou E, Patel VC, Weston CJ, et al. Patients with acute-on-chronic liver failure have increased numbers of regulatory immune cells expressing the receptor tyrosine kinase MERTK. Gastroenterology 2015;148:603–615 e14.
[34] O'Neill LA, Kishton RJ, Rathmell J. A guide to immunometabolism for immunologists. Nat Rev Immunol 2016;16:553–565.
[35] Kelly B, O'Neill LA. Metabolic reprogramming in macrophages and dendritic cells in innate immunity. Cell Res 2015;25:771–784.
[36] Nakajima T. Roles of sulfur metabolism and rhodanese in detoxification and anti-oxidative stress functions in the liver: responses to radiation exposure. Med Sci Monit 2015;21:1721–1725.
[37] Juanola A, Graupera I, Elia C, Piano S, Sole C, Carol M, et al. Urinary L-FABP is a promising prognostic biomarker of ACLF and mortality in patients with decompensated cirrhosis. J Hepatol 2022;76:107–114.
[38] **Ariza X**, **Graupera I**, Coll M, Sola E, Barreto R, Garcia E, et al. Neutrophil gelatinase-associated lipocalin is a biomarker of acute-on-chronic liver failure and prognosis in cirrhosis. J Hepatol 2016;65:57–65.
[39] **Helmy KY**, **Katschke KJ**, Gorgani NN, Kljavin NM, Elliott JM, Diehl L, et al. CRIg: a macrophage complement receptor required for phagocytosis of circulating pathogens. Cell 2006;124:915–927.
[40] Jung K, Kang M, Park C, Hyun Choi Y, Jeon Y, Park SH, et al. Protective role of V-set and immunoglobulin domain-containing 4 expressed on kupffer cells during immune-mediated liver injury by inducing tolerance of liver T- and natural killer T-cells. Hepatology 2012;56:1838–1848.
[41] Li J, Diao B, Guo S, Huang X, Yang C, Feng Z, et al. VSIG4 inhibits proinflammatory macrophage activation by reprogramming mitochondrial pyruvate metabolism. Nat Commun 2017;8:1322.
[42] Irvine KM, Banh X, Gadd VL, Wojcik KK, Ariffin JK, Jose S, et al. CRIg-expressing peritoneal macrophages are associated with disease severity in patients with cirrhosis and ascites. JCI Insight 2016;1:e86914.
[43] Reissing J, Lutz P, Frissen M, Ibidapo-Obe O, Reuken PA, Wirtz TH, et al. Immunomodulatory receptor VSIG4 is released during spontaneous bacterial peritonitis and predicts short-term mortality. JHEP Rep 2022;4:100391.
[44] Lieberman LA, Mizui M, Nalbandian A, Bosse R, Crispin JC, Tsokos GC. Complement receptor of the immunoglobulin superfamily reduces murine lupus nephritis and cutaneous disease. Clin Immunol 2015;160:286–291.
[45] Vogt L, Schmitz N, Kurrer MO, Bauer M, Hinton HI, Behnke S, et al. VSIG4, a B7 family-related protein, is a negative regulator of T cell activation. J Clin Invest 2006;116:2817–2826.
[46] Eisfeld AJ, Halfmann PJ, Wendler JP, Kyle JE, Burnum-Johnson KE, Peralta Z, et al. Multi-platform 'omics analysis of human ebola virus disease pathogenesis. Cell Host Microbe 2017;22:817–829 e8.
[47] Wiesmann C, Katschke KJ, Yin J, Helmy KY, Steffek M, Fairbrother WJ, et al. Structure of C3b in complex with CRIg gives insights into regulation of complement activation. Nature 2006;444:217–220.